PHYSICAL REVIEW D **89,** 061701(R) (2014)

Three-loop pressure and susceptibility at finite temperature and density from hard-thermal-loop perturbation theory

Najmul Haque,[1] Jens O. Andersen,[2] Munshi G. Mustafa,[3] Michael Strickland,[4] and Nan Su[5]

[1]*Theory Division, Saha Institute of Nuclear Physics, Kolkata, India 700064*
[2]*Department of Physics, Norwegian University of Science and Technology, N-7491 Trondheim, Norway*
[3]*Theory Division, Saha Institute of Nuclear Physics, Kolkata, India 700064*
[4]*Physics Department, Kent State University, Kent, Ohio 44242, USA*
[5]*Faculty of Physics, University of Bielefeld, D-33615 Bielefeld, Germany*

(Received 2 October 2013; revised manuscript received 12 November 2013; published 6 March 2014)

We present results of a three-loop hard-thermal-loop perturbation theory calculation of the thermodynamical potential of a finite temperature and baryon chemical potential system of quarks and gluons. We compare the resulting pressure and diagonal quark susceptibilities with available lattice data. We find reasonable agreement between our analytic results and lattice data at both zero and finite chemical potential.

DOI: 10.1103/PhysRevD.89.061701 PACS numbers: 11.15.Bt, 04.25.Nx, 11.10.Wx, 12.38.Mh

I. INTRODUCTION

A comprehensive understanding of the quantum chromodynamics (QCD) equation of state is of crucial importance for a better understanding of the matter created in ultrarelativistic heavy-ion collisions [1], as well as the candidates for dark matter in cosmology [2]. The calculation of QCD thermodynamics utilizing weakly coupled quantum field theory has a long history [3–5]. The perturbative pressure is known up to order $g_s^6 \log g_s$, where g_s is the strong-coupling constant [5]. Unfortunately, a straightforward application of perturbation theory is of limited use since the weak-coupling expansion does not converge unless the temperature is extraordinarily high. Comparing the magnitude of low-order contributions to the QCD free energy with three quark flavors ($N_f = 3$), one finds that the g_s^3 contribution is smaller than the g_s^2 contribution only for $g_s \lesssim 0.9$ or $\alpha_s \lesssim 0.07$, which corresponds to a temperature of $T \sim 10^5$ GeV $\sim 5 \times 10^5 T_c$, with $T_c \sim 175$ MeV being the QCD pseudocritical temperature.

The poor convergence of the weak-coupling expansion of thermodynamic functions stems from the fact that at high temperatures the classical solution is not well described by massless degrees of freedom, and is instead better described by massive quasiparticles with nontrivial dispersion relations and interactions. One way to deal with the problem is to use an effective field theory framework in which one treats hard modes using standard four-dimensional QCD and soft modes using a dimensionally reduced three-dimensional SU(3) plus adjoint Higgs model [5–7], but treating the soft sector nonperturbatively by not expanding the soft contributions in powers of the coupling constant [5,8]. The technique of treating the soft sector nonperturbatively is ubiquitous and there exist several ways of systematically reorganizing the perturbative series at finite temperature which rely on improved treatment of the soft sector (see e.g. [9,10]). Such treatments are based on a quasiparticle picture in which one performs a loop expansion around an ideal gas of massive quasiparticles, rather than an ideal gas of massless particles.

In this paper we present results for the finite-temperature and density next-to-next-to-leading-order (NNLO) QCD pressure and diagonal quark susceptibilities obtained using the hard-thermal-loop perturbation theory (HTLpt) reorganization [11–14] of finite-temperature/density QCD. This work extends previous NNLO work at zero chemical potential [14] and previous leading-order (LO) [15–17] and next-to-leading-order (NLO) work at finite chemical potential [18] to NNLO. For our results we present (i) comparisons of the pressure scaled by the ideal pressure to available lattice data at zero and finite chemical potential and (ii) comparisons of the extracted second- and fourth-order diagonal quark number susceptibilities to available lattice data. We present the explicit analytic expression for the NNLO HTLpt thermodynamic potential in the Appendix.

II. HTLPT FORMAL SETUP

The Minkowski space Lagrangian density for an SU(N_c) Yang-Mills theory with N_f massless fermions is

$$\mathcal{L}_{\rm QCD} = -\frac{1}{2}\,{\rm Tr}\,[G_{\mu\nu}G^{\mu\nu}] + i\bar{\psi}\gamma^\mu D_\mu \psi + \mathcal{L}_{gf} + \mathcal{L}_{gh} + \Delta\mathcal{L}_{\rm QCD}, \tag{1}$$

where the field strength is $G^{\mu\nu} = \partial^\mu A^\nu - \partial^\nu A^\mu - ig_s[A^\mu, A^\nu]$ and the covariant derivative is $D^\mu = \partial^\mu - ig_s A^\mu$. $\Delta\mathcal{L}_{\rm QCD}$ contains the counterterms necessary to cancel ultraviolet divergences in perturbative calculations. The ghost term $\mathcal{L}_{\rm gh}$ depends on the gauge-fixing term $\mathcal{L}_{\rm gf}$. In this paper we work in the general covariant gauge where $\mathcal{L}_{\rm gf} = -\xi^{-1}\,{\rm Tr}\,[(\partial_\mu A^\mu)^2]$ with ξ being the gauge-fixing parameter.

As mentioned previously, HTLpt is a reorganization of the perturbation series for thermal QCD. The Lagrangian

density is written as $\mathcal{L} = (\mathcal{L}_{\rm QCD} + \mathcal{L}_{\rm HTL})|_{g_s \to \sqrt{\delta} g_s} + \Delta\mathcal{L}_{\rm HTL}$, where $\Delta\mathcal{L}_{\rm HTL}$ contains the additional counterterms necessary to cancel the ultraviolet divergences introduced by HTLpt. HTLpt is gauge invariant order-by-order in the dressed-loop expansion, and consequently, the results obtained are independent of the gauge-fixing parameter ξ. In Ref. [12], the gauge-fixing parameter independence in general Coulomb and covariant gauges was explicitly demonstrated. We use $\overline{\rm MS}$ dimensional regularization with a renormalization scale Λ introduced to regularize infrared and ultraviolet divergences. The HTL improvement term is

$$\mathcal{L}_{\rm HTL} = -\frac{1}{2}(1-\delta) m_D^2 \,{\rm Tr}\left(G_{\mu\alpha} \left\langle \frac{y^\alpha y^\beta}{(y\cdot D)^2} \right\rangle_y G^\mu{}_\beta \right) + (1-\delta) i m_q^2 \bar{\psi} \gamma^\mu \left\langle \frac{y_\mu}{y\cdot D} \right\rangle_y \psi, \tag{2}$$

where $y^\mu = (1, \hat{\mathbf{y}})$ is a lightlike four-vector and $\langle \ldots \rangle_y$ represents an average over the directions specified by the three-dimensional unit vector $\hat{\mathbf{y}}$. The parameters m_D and m_q can be identified with the Debye screening mass and the fermion thermal mass in the weak-coupling limit; however, in HTLpt they are treated as free parameters to be fixed at the end of the calculation. The parameter δ is the formal expansion parameter: HTLpt is defined as an expansion in powers of δ around $\delta = 0$, followed by taking $\delta \to 1$. This expansion systematically generates dressed propagators and vertices with expansions to order δ^0, δ^1, and δ^2 corresponding to LO, NLO, and NNLO, respectively.

Through inclusion of the HTL improvement term (2), HTLpt systematically shifts the perturbative expansion from being around an ideal gas of massless particles, which is the physical picture of the naive weak-coupling expansion, to being around a gas of massive quasiparticles. Since the loop expansion is an expansion around the classical extremum of the action, this shift incorporates the classical physics of the high-temperature quark gluon plasma, i.e. Debye screening and Landau damping, from the outset and loop corrections correspond to true quantum and thermal corrections to the classical high temperature limit. In addition, new vertices which account for in-medium HTL interactions are self-consistently generated in the HTLpt framework.

There is no general proof that the HTLpt expansion is renormalizable and, as a result, the general structure of the ultraviolet divergences is unknown. However, in practice it has been explicitly demonstrated in Refs. [12–14] that it is possible to renormalize the HTLpt thermodynamic potential using only a vacuum counterterm, a Debye mass counterterm, a fermion mass counterterm, and a coupling constant counterterm. Through $\mathcal{O}(\delta^2)$ the HTLpt counterterms necessary to renormalize the thermodynamic potential are

$$\delta\Delta\alpha_s = -\frac{11c_A - 4s_F}{12\pi\epsilon}\alpha_s^2\delta^2, \tag{3}$$

$$\Delta m_D^2 = \left(-\frac{11c_A - 4s_F}{12\pi\epsilon}\alpha_s\delta\right)(1-\delta)m_D^2, \tag{4}$$

$$\Delta m_q^2 = \left(-\frac{3}{8\pi\epsilon}\frac{d_A}{c_A}\alpha_s\delta\right)(1-\delta)m_q^2, \tag{5}$$

$$\Delta\mathcal{E}_0 = \left(\frac{d_A}{128\pi^2\epsilon}\right)(1-\delta)^2 m_D^4, \tag{6}$$

where $c_A = N_c$, $d_A = N_c^2 - 1$, and $s_F = N_f/2$.

In practice, in addition to the δ expansion, it is also necessary to make a Taylor expansion in the mass parameters scaled by the temperature, m_D/T and m_q/T, in order to obtain analytically tractable sum-integrals. Otherwise, one would have to resort to numerical evaluation and regularization of difficult multidimensional sum-integrals. An added benefit of this procedure is that the final result obtained at NNLO is completely analytic. In order to truncate the series in m_D/T and m_q/T one treats these quantities as being $\mathcal{O}(g_s)$ at leading order, keeping all terms that naively contribute to the thermodynamic potential through $\mathcal{O}(g_s^5)$. In practice, such a truncated expansion works well [17,19] and the radius of convergence of the scaled mass expansion seems to be quite large, giving us confidence in this approximate treatment of the necessary sum-integrals.

III. RESULTS

We present the full analytic expression for the NNLO HTLpt result in Eq. (A1) in the Appendix. In this section we collect plots of the results and compare them to lattice data. For all results we use the Braaten-Nieto mass prescription for the gluon Debye mass specified in Eq. (A2) and choose $m_q = 0$ since this is the self-consistent solution to the quark gap equation at NNLO (see Ref. [14] for a discussion of gluon and quark mass prescriptions within NNLO HTLpt). For the strong-coupling constant α_s, we use one-loop running [20] with $\Lambda_{\overline{\rm MS}} = 176$ MeV, which for $N_f = 3$ gives $\alpha_s(1.5\ {\rm GeV}) = 0.326$ [21] which is the self-consistent running obtained in NNLO HTLpt. We use separate renormalization scales, Λ_g and Λ_q, for pure-glue and fermionic graphs, respectively. We take the central values of these renormalization scales to be $\Lambda_g = 2\pi T$ and $\Lambda_q = 2\pi\sqrt{T^2 + \mu^2/\pi^2}$ in all figures. This choice of scales guarantees that the quark susceptibility vanishes in the limit $N_f \to 0$. In all figures, the black line indicates the result obtained using these central values. The variation when changing these scales by a factor of 2 around the central values is indicated by a shaded band.

In Figs. 1 and 2, we show the normalized pressure for $N_c = 3$ and $N_f = 2 + 1$ as a function of T, for $\mu_B = 0$ and $\mu_B = 400$ MeV, respectively [22]. The result shown in

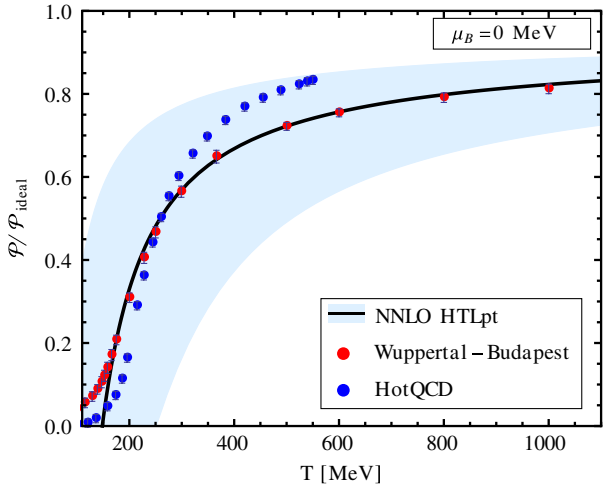

FIG. 1 (color online). Comparison of the $\mu_B = 0$ NNLO HTLpt result for the scaled pressure for $N_f = 2 + 1$ with lattice data from Bazavov *et al.* [23] and Borsanyi *et al.* [24].

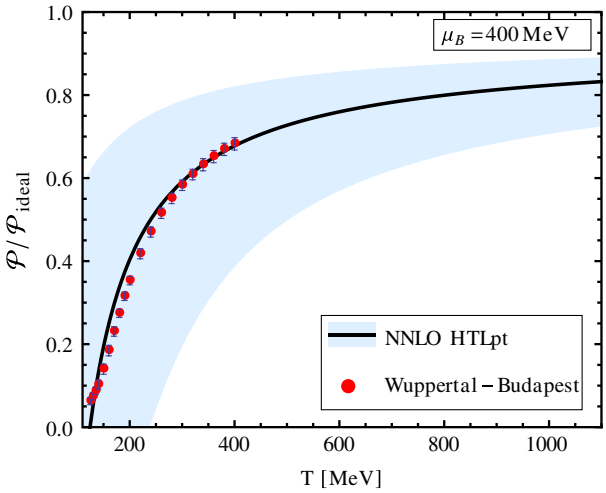

FIG. 2 (color online). Comparison of the $\mu_B = 400$ MeV NNLO HTLpt result for the scaled pressure for $N_f = 2 + 1$ with lattice data from Borsanyi *et al.* [25].

Fig. 1 has been published previously (see Ref. [14]); however, we present it here for completeness and comparison with the finite density case. Figure 2 is our first new result. As can be seen from Figs. 1 and 2, the central (black) line agrees quite well with both the $\mu_B = 0$ and $\mu_B = 400$ MeV lattice data with no parameters being fit. The deviations below $T \sim 200$ MeV are due to the fact that our calculation does not include hadronic degrees of freedom which dominate at low temperatures (see e.g. fits in [26]) or nonperturbative effects [27].

In Fig. 3, we present the difference of the pressure at finite chemical potential and zero chemical potential, $\Delta\mathcal{P} \equiv \mathcal{P}(T, \mu_B) - \mathcal{P}(T, \mu_B = 0)$, as a function of the temperature for $\mu_B = 300$ MeV and $\mu_B = 400$ MeV. The solid lines are the NNLO HTLpt result and the dashed lines

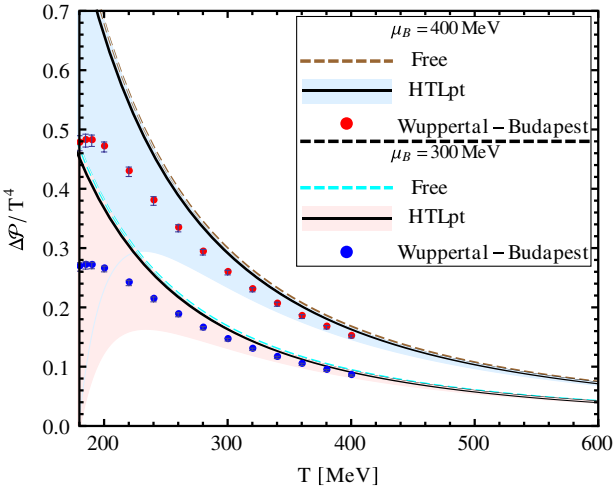

FIG. 3 (color online). Comparison of the Stefan-Boltzmann limit (dashed lines) and NNLO HTLpt (solid lines) results for the scaled pressure difference $\Delta\mathcal{P} \equiv \mathcal{P}(T, \mu_B) - \mathcal{P}(T, \mu_B = 0)$ with $N_f = 2 + 1$ lattice data from Borsanyi *et al.* [25].

are the result obtained in the Stefan-Boltzmann limit. We note that in Fig. 3 the lattice data from the Wuppertal-Budapest (WB) are computed up to $\mathcal{O}(\mu_B^2)$, whereas the HTLpt result includes all orders in μ_B. As can be seen from Fig. 3, the NNLO HTLpt result is quite close to the result obtained in the Stefan-Boltzmann limit. The NNLO HTLpt result, however, is in better agreement with the available lattice data. Note that the small correction in going from the Stefan-Boltzmann limit to NNLO HTLpt indicates that the fermionic sector is, to a good approximation, weakly coupled for $T \gtrsim 2T_c$.

As a more sensitive measure of the dependence of the pressure on the chemical potential, one can calculate the diagonal quark number susceptibilities (QNS). The diagonal nth order QNS is

$$\chi_n^i(T) \equiv \left.\frac{\partial^n \mathcal{P}}{\partial \mu_i^n}\right|_{\mu_i = 0}, \tag{7}$$

where $\mathcal{P}$ is the pressure of system, T is the temperature, and μ_i is a chemical potential associated with conserved charge $i \in \{B, Q, S\}$ corresponding to baryon number, electric charge, and strangeness, respectively [28]. We begin by noting that since the NNLO HTLpt result (A1) was obtained assuming equal chemical potentials for N_f massless quark flavors ($\mu = \mu_B/3$ and $\mu_Q = \mu_S = 0$), derivatives of the result with respect to μ are related to the diagonal baryon number susceptibility.

In Figs. 4 and 5, we compare the second- and fourth-order susceptibilities predicted by NNLO HTLpt with available lattice data. In Fig. 4, the data labeled WB, BNL-BI(B), BNL-BI(u,s), TIFR, and MILC come from Refs. [29–33], respectively. In Fig. 5, the data labeled BNL-BI and WB come from Refs. [30] and [34], respectively. We

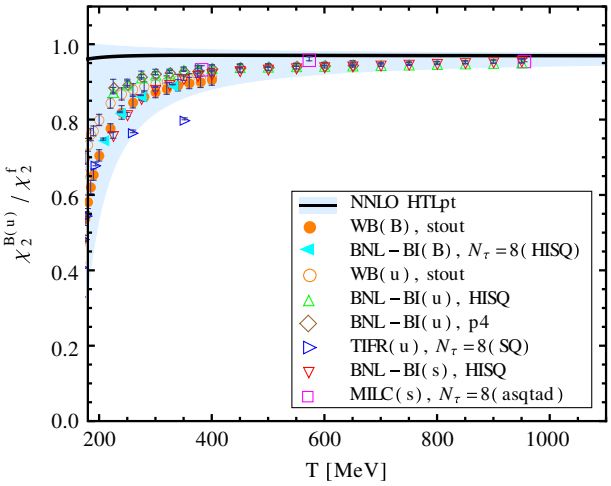

FIG. 4 (color online). Comparison of the NNLO HTLpt result for the scaled second-order susceptibility with lattice data.

have indicated the action used in each case in the legend, and sets without a value of N_τ specified are continuum-extrapolated results. We note that for χ_2 the largest N_τ results are in quite good agreement with the continuum-extrapolated results. Additionally, we note that the HTLpt bands shown are predominantly due to the variation of the central scales to one half of their central values.

For the second-order susceptibility, we compare with lattice results for both single flavor (u, s) and baryon number susceptibilities (B). For the fourth-order susceptibility, we show only lattice results for the fourth-order baryon number susceptibility. It is expected that the second-order single flavor and baryon number susceptibilities differ only at the percent level because of small off-diagonal contributions; however, the fourth-order single flavor and baryon number susceptibilities are

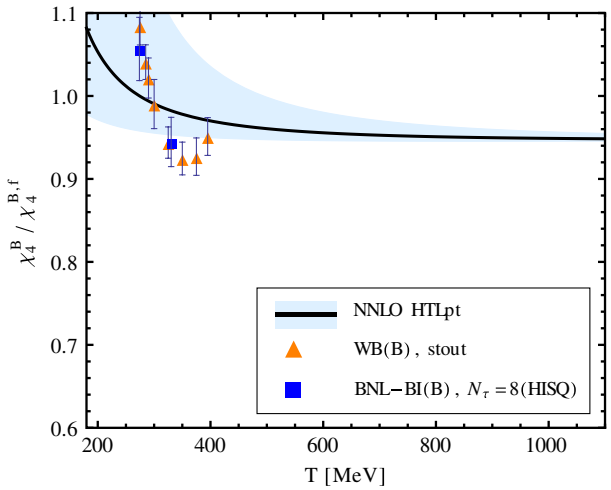

FIG. 5 (color online). Comparison of the NNLO HTLpt result for the scaled fourth-order susceptibility with lattice data.

expected to differ by approximately 20% near the phase transition [35].

As can be seen from Fig. 4, the agreement between NNLO HTLpt and lattice data for the second-order baryon-number susceptibility is quite reasonable at high temperatures. In addition, we note that in the case of the second-order susceptibility, the LO [15–17] and NLO [18] HTLpt predictions are close to the NNLO result shown in Fig. 4, indicating that this quantity converges nicely in HTLpt. The fourth-order susceptibility, however, shows a significant change in going from LO to NLO to NNLO (see Fig. 2 of Ref. [18] for the LO and NLO results). This is due to the fact that the fourth-order susceptibility is very sensitive to overcounting which occurs in low-order HTLpt. At NNLO this overcounting is fixed through order g_s^5 if the result is perturbatively expanded. As can be seen from Fig. 5, the NNLO HTLpt result seems to be in reasonable agreement with the lattice measurements of χ_4^B.

IV. CONCLUSIONS

In this paper we presented results for the NNLO HTLpt QCD pressure with an arbitrary number of colors and quark flavors. The final result is completely analytic and when its predictions are compared with available lattice data, one finds reasonable agreement for the pressure and second- and fourth-order diagonal susceptibilities down to temperatures on the order of $T \sim 2T_c$. The analytic result obtained is gauge invariant and, besides the choice of the renormalization scales Λ_g and Λ_q, does not contain any free fit parameters. Details concerning the calculation of the NNLO results listed in Eqs. (A1) and (A2) are presented elsewhere [36]. In closing, we note that the application of hard thermal loops in the heavy ion phenomenology is ubiquitous, and the fact that HTLpt is able to reproduce the finite temperature and chemical potential thermodynamic functions with reasonable accuracy offers some hope that the application of this method to the computation of other processes or quantities is warranted.

ACKNOWLEDGMENTS

We thank S. Borsányi, S. Datta, F. Karsch, S. Gupta, P. Petreczky, S. Mogliacci, and A. Vuorinen for useful discussions. M. S. was supported in part by DOE Grant No. DE-SC0004104. N. S. was supported by a Postdoctoral Research Fellowship from the Alexander von Humboldt Foundation.

APPENDIX: NNLO HTLPT THERMODYNAMIC POTENTIAL

In this appendix we present the NNLO HTLpt thermodynamic potential

$$\frac{\Omega_{\rm NNLO}}{\Omega_0}=\frac{7}{4}\frac{d_F}{d_A}\left(1+\frac{120}{7}\hat{\mu}^2+\frac{240}{7}\hat{\mu}^4\right)+\frac{s_F\alpha_s}{\pi}\left[-\frac{5}{8}(1+12\hat{\mu}^2)(5+12\hat{\mu}^2)+\frac{15}{2}(1+12\hat{\mu}^2)\hat{m}_D\right.$$
$$\left.+\frac{15}{2}\left(2\ln\frac{\hat{\Lambda}_q}{2}-1-\aleph(z)\right)\hat{m}_D^3-90\hat{m}_q^2\hat{m}_D\right]+s_{2F}\left(\frac{\alpha_s}{\pi}\right)^2\left[\frac{15}{64}\left\{35-32(1-12\hat{\mu}^2)\frac{\zeta'(-1)}{\zeta(-1)}+472\hat{\mu}^2\right.\right.$$
$$\left.\left.+1328\hat{\mu}^4+64(-36i\hat{\mu}\aleph(2,z)+6(1+8\hat{\mu}^2)\aleph(1,z)+3i\hat{\mu}(1+4\hat{\mu}^2)\aleph(0,z))\right\}-\frac{45}{2}\hat{m}_D(1+12\hat{\mu}^2)\right]$$
$$+\left(\frac{s_F\alpha_s}{\pi}\right)^2\left[\frac{5}{4\hat{m}_D}(1+12\hat{\mu}^2)^2+30(1+12\hat{\mu}^2)\frac{\hat{m}_q^2}{\hat{m}_D}+\frac{25}{12}\left\{\left(1+\frac{72}{5}\hat{\mu}^2+\frac{144}{5}\hat{\mu}^4\right)\ln\frac{\hat{\Lambda}_q}{2}\right.\right.$$
$$+\frac{1}{20}(1+168\hat{\mu}^2+2064\hat{\mu}^4)+\frac{3}{5}(1+12\hat{\mu}^2)^2\gamma_E-\frac{8}{5}(1+12\hat{\mu}^2)\frac{\zeta'(-1)}{\zeta(-1)}-\frac{34}{25}\frac{\zeta'(-3)}{\zeta(-3)}$$
$$-\frac{72}{5}[8\aleph(3,z)+3\aleph(3,2z)-12\hat{\mu}^2\aleph(1,2z)+12i\hat{\mu}(\aleph(2,z)+\aleph(2,2z))-i\hat{\mu}(1+12\hat{\mu}^2)\aleph(0,z)$$
$$\left.\left.-2(1+8\hat{\mu}^2)\aleph(1,z)]\right\}-\frac{15}{2}(1+12\hat{\mu}^2)\left(2\ln\frac{\hat{\Lambda}_q}{2}-1-\aleph(z)\right)\hat{m}_D\right]$$
$$+\left(\frac{c_A\alpha_s}{3\pi}\right)\left(\frac{s_F\alpha_s}{\pi}\right)\left[\frac{15}{2\hat{m}_D}(1+12\hat{\mu}^2)-\frac{235}{16}\left\{\left(1+\frac{792}{47}\hat{\mu}^2+\frac{1584}{47}\hat{\mu}^4\right)\ln\frac{\hat{\Lambda}_q}{2}-\frac{144}{47}(1+12\hat{\mu}^2)\ln\hat{m}_D\right.\right.$$
$$+\frac{319}{940}\left(1+\frac{2040}{319}\hat{\mu}^2+\frac{38640}{319}\hat{\mu}^4\right)-\frac{24\gamma_E}{47}(1+12\hat{\mu}^2)-\frac{44}{47}\left(1+\frac{156}{11}\hat{\mu}^2\right)\frac{\zeta'(-1)}{\zeta(-1)}-\frac{268}{235}\frac{\zeta'(-3)}{\zeta(-3)}$$
$$\left.\left.-\frac{72}{47}[4i\hat{\mu}\aleph(0,z)+(5-92\hat{\mu}^2)\aleph(1,z)+144i\hat{\mu}\aleph(2,z)+52\aleph(3,z)]\right\}+90\frac{\hat{m}_q^2}{\hat{m}_D}+\frac{315}{4}\left\{\left(1+\frac{132}{7}\hat{\mu}^2\right)\ln\frac{\hat{\Lambda}_q}{2}\right.$$
$$\left.+\frac{11}{7}(1+12\hat{\mu}^2)\gamma_E+\frac{9}{14}\left(1+\frac{132}{9}\hat{\mu}^2\right)+\frac{2}{7}\aleph(z)\right\}\hat{m}_D\Big]+\frac{\Omega^{\rm YM}_{\rm NNLO}(\Lambda_g)}{\Omega_0}. \tag{A1}$$

The last term above is the scaled pure-glue pressure, $\Omega^{\rm YM}_{\rm NNLO}$, which can be found in Ref. [13]. For the gluon Debye mass we use the Braaten-Nieto prescription [4,13,14] extended to finite chemical potential

$$\hat{m}_D^2=\frac{\alpha_s}{3\pi}\left\{c_A+\frac{c_A^2\alpha_s}{12\pi}\left(5+22\gamma_E+22\ln\frac{\hat{\Lambda}_g}{2}\right)+s_F(1+12\hat{\mu}^2)+\frac{c_As_F\alpha_s}{12\pi}((9+132\hat{\mu}^2)+22(1+12\hat{\mu}^2)\gamma_E\right.$$
$$\left.+2(7+132\hat{\mu}^2)\ln\frac{\hat{\Lambda}_q}{2}+4\aleph(z))+\frac{s_F^2\alpha_s}{3\pi}(1+12\hat{\mu}^2)\left(1-2\ln\frac{\hat{\Lambda}_q}{2}+\aleph(z)\right)-\frac{3}{2}\frac{s_{2F}\alpha_s}{\pi}(1+12\hat{\mu}^2)\right\}. \tag{A2}$$

In Eqs. (A1) and (A2) $\Omega_0\equiv -d_A\pi^2T^4/45$, $z=1/2-i\hat{\mu}$, $\hat{m}_D=m_D/2\pi T$, $\hat{\mu}=\mu/2\pi T$, $\hat{\Lambda}_{g,q}=\Lambda_{g,q}/2\pi T$, and

$$\aleph(n,z)\equiv\zeta'(-n,z)+(-1)^{n+1}\zeta'(-n,z^*),\qquad \aleph(z)\equiv\Psi(z)+\Psi(z^*),\qquad \zeta'(x,y)\equiv\partial_x\zeta(x,y). \tag{A3}$$

Above, ζ is the Riemann zeta function, Ψ is the digamma function, and n is a non-negative integer. With the standard normalization, we have $c_A=N_c$, $d_A=N_c^2-1$, $s_F=N_f/2$, $d_F=N_cN_f$, and $s_{2F}=(N_c^2-1)N_f/4N_c$.

[1] I. Arsene *et al.*, Nucl. Phys. **A757**, 1 (2005); B. B. Back *et al.* Nucl. Phys. **A757**, 28 (2005); J. Adams *et al.* Nucl. Phys. **A757**, 102 (2005); K. Adcox *et al.* Nucl. Phys. **A757**, 184 (2005); K. Aamodt *et al.* Phys. Rev. Lett. **105**, 252302 (2010); S. Chatrchyan *et al.* Phys. Rev. C **87**, 014902 (2013); M. Gyulassy and L. McLerran Nucl. Phys. **A750**, 30 (2005).

[2] M. Hindmarsh and O. Philipsen, Phys. Rev. D **71**, 087302 (2005); M. Laine *Proc. Sci.*, LAT2006 (**2006**) 014.

[3] [E. V. ShuryakSov. Phys. JETP **47**, 212 (1978) [Zh. Eksp. Teor. Fiz. **74**, 408 (1978)]; J. I. Kapusta Nucl. Phys. **B148** 461 (1979). T. Toimela Int. J. Theor. Phys. **24**, 901 (1985); **26**, 1021(E) (1987); P. Arnold and C. X. Zhai Phys. Rev. D **50**, 7603 (1994); **51**, 1906 (1995); C. X. Zhai and

B. Kastening Phys. Rev. D **52**, 7232 (1995);E. Braaten and A. Nieto Phys. Rev. Lett. **76**, 1417 (1996); **53**, 3421 (1996); A. Vuorinen Phys. Rev. D **67**, 074032 (2003); **68**, 054017 (2003); A. Rebhan hep-ph/0301130; A. Ipp K. Kajantie, A. Rebhan, and A. Vuorinen, Phys. Rev. D **74**, 045016 (2006).

[4] E. Braaten and A. Nieto, Phys. Rev. Lett. **76**, 1417 (1996); Phys. Rev. D **53**, 3421 (1996).

[5] K. Kajantie, M. Laine, K. Rummukainen, and Y. Schröder, Phys. Rev. D **67**, 105008 (2003).

[6] A. Hietanen, K. Kajantie, M. Laine, K. Rummukainen, and Y. Schroder, Phys. Rev. D **79**, 045018 (2009).

[7] M. Laine and Y. Schroder, Phys. Rev. D **73**, 085009 (2006).

[8] J. P. Blaizot, E. Iancu, and A. Rebhan, Phys. Rev. D **68**, 025011 (2003).

[9] J. P. Blaizot, E. Iancu, and A. Rebhan, in *Quark Gluon Plasma*, edited by R. C. Hwa and X.-N. Wang (World Scientific, Singapore, 2004), p. 60; U. Kraemmer and A. Rebhan Rep. Prog. Phys. **67**, 351 (2004); J. O. Andersen and M. Strickland Ann. Phys. (Amsterdam) **317**, 281 (2005); N. Su Commun. Theor. Phys. **57**, 409 (2012).

[10] F. Karsch, A. Patkos, and P. Petreczky, Phys. Lett. B **401**, 69 (1997); S. Chiku and T. Hatsuda Phys. Rev. D **58**, 076001 (1998); J. O. Andersen E. Braaten, and M. Strickland, Phys. Rev. D **63**, 105008 (2001).

[11] E. Braaten and R. D. Pisarski, Phys. Rev. D **45**, R1827 (1992).

[12] J. O. Andersen, E. Braaten, E. Petitgirard, and M. Strickland, Phys. Rev. D **66**, 085016 (2002); J. O. Andersen E. Petitgirard, and M. Strickland, Phys. Rev. D **70**, 045001 (2004).

[13] J. O. Andersen, M. Strickland, and N. Su, Phys. Rev. Lett. **104**, 122003 (2010); J. High Energy Phys. 08 (2010) 113.

[14] J. O. Andersen, L. E. Leganger, M. Strickland, and N. Su, Phys. Lett. B **696**, 468 (2011); Phys. Rev. D **84**, 087703 (2011); 08 (2011) 053.

[15] P. Chakraborty, M. G. Mustafa, and M. H. Thoma, Eur. Phys. J. C **23**, 591 (2002); Phys. Rev. D **68**, 085012 (2003); N. Haque M. G. Mustafa, and M. H. Thoma, Phys. Rev. D **84**, 054009 (2011); N. Haque and M. G. Mustafa Nucl. Phys. **A862**, 271 (2011); N. Haque and M. G. Mustafa arXiv:1007.2076.

[16] J. O. Andersen, S. Mogliacci, N. Su, and A. Vuorinen, Phys. Rev. D **87**, 074003 (2013).

[17] S. Mogliacci, J. O. Andersen, M. Strickland, N. Su, and A. Vuorinen, J. High Energy Phys. 12 (2013) 055.

[18] N. Haque, M. G. Mustafa, and M. Strickland, Phys. Rev. D **87**, 105007 (2013); J. High Energy Phys. 07 (2013) 184.

[19] J. O. Andersen and M. Strickland, Phys. Rev. D **64**, 105012 (2001).

[20] J. Beringer *et al.* (Particle Data Group), Phys. Rev. D **86**, 010001 (2012).

[21] A. Bazavov, N. Brambilla, X. Garcia i Tormo, P. Petreczky, J. Soto, and A. Vairo, Phys. Rev. D **86**, 114031 (2012).

[22] Our calculation assumes vanishing bare quark masses. For a comparison with $2+1$ lattice data, we use $N_f = 3$.

[23] A. Bazavov *et al.*, Phys. Rev. D **80**, 014504 (2009).

[24] S. Borsanyi, G. Endrődi, Z. Fodor, A. Jakovác, S. D. Katz, S. Krieg, C. Ratti, and K. K. Szabó, J. High Energy Phys. 11 (2010) 077.

[25] Sz. Borsanyi, G. Endrődi, Z. Fodor, S. D. Katz, S. Krieg, C. Ratti, and K. K. Szabó, J. High Energy Phys. 08 (2012) 053.

[26] P. Huovinen and P. Petreczky, Nucl. Phys. **A837**, 26 (2010).

[27] C. Korthals-Altes, A. Kovner, and M. A. Stephanov, Phys. Lett. B **469**, 205 (1999); C. Korthals-Altes and A. Kovner Phys. Rev. D **62**, 096008 (2000); R. D. Pisarski Phys. Rev. D **62**, 111501 (2000); A. Vuorinen and L. G. Yaffe Phys. Rev. D **74**, 025011 (2006); Ph. de Forcrand A. Kurkela, and A. Vuorinen, Phys. Rev. D **77**, 125014 (2008); D. Zwanziger Phys. Rev. Lett. **94**, 182301 (2005); K. Fukushima and N. Su Phys. Rev. D **88**, 076008 (2013).

[28] When taking derivatives of Eq. (A1) with respect to μ, we include the μ and T dependence of the RG-scale Λ only after the derivatives are taken.

[29] S. Borsanyi, Z. Fodor, S. D. Katz, S. Krieg, C. Ratti, and K. Szabó *et al.*, J. High Energy Phys. 01 (2012) 138.

[30] A. Bazavov *et al.*, Phys. Rev. Lett. **111**, 082301 (2013).

[31] A. Bazavov, H.-T. Ding, P. Hegde, F. Karsch, C. Miao, Swagato Mukherjee, P. Petreczky, C. Schmidt, and A. Velytsky, Phys. Rev. D **88**, 094021 (2013).

[32] S. Datta, R. V. Gavai, and S. Gupta, http://www.ilgti.tifr.res.in/tables (to be published).

[33] C. Bernard, T. Burch, C. DeTar, J. Osborn, Steven Gottlieb, E. Gregory, D. Toussaint, U. Heller, and R. Sugar, Phys. Rev. D **71**, 034504 (2005).

[34] S. Borsanyi, Nucl. Phys. **A904**, 270c (2013).

[35] F. Karsch and P. Petreczky (private communication).

[36] N. Haque *et al.* (unpublished).